Inorganic Chemistry

Article

pubs.acs.org/IC

Energetics of Order–Disorder in Layered Magnesium Aluminum Double Hydroxides with Interlayer Carbonate

Radha Shivaramaiah and Alexandra Navrotsky*

Peter A. Rock Thermochemistry Laboratory and NEAT ORU, University of California Davis, Davis, California 95616, United States

Supporting Information

ABSTRACT: Laboratory synthesis of layered double hydroxides (LDH) often results in materials replete with stacking faults. Faults are known to affect several properties including sorption, electrochemical, and catalytic activity of this important class of materials. Understanding the occurrence of faults thus calls for a comprehensive analysis of formation and stability of ordered and faulted LDHs. High-temperature oxide melt solution calorimetric measurements made on an ordered and a faulted Mg–Al LDH with carbonate interlayer anion shows that ordered LDH is energetically more stable than the faulted one by ~6 kJ/mol. The stacking faults are an intergrowth of $3R_1$ and $2H_1$ polytypes, and faults could thus mediate transformation of $3R_1$ to $2H_1$ polytypes. Several factors including pH and temperature of precipitation also affect layer stacking. The formation of stacking faults could therefore have its origin in kinetics. Water content in the interlayer also affects layer stacking, and hence it may affect properties of LDH. Improved understanding of the distribution of water molecules in LDH is also crucial in an environmental context, as LDH occur as minerals and are important for contaminant amelioration in the environment. Water adsorption calorimetry on dehydrated LDH shows a continuous decrease in the magnitude of adsorption enthalpy with increasing coverage, indicating the presence of energetically heterogeneous sites where the water molecules reside. The results also indicate that the energy of several sites where the water molecules may reside (whether in the interlayer or on the surface) overlaps, and hence it is hard to differentiate among them.

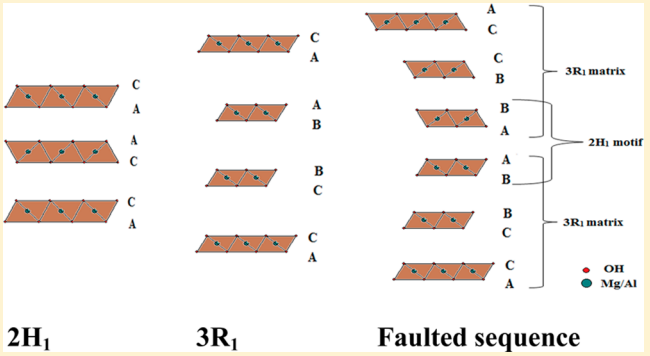

INTRODUCTION

Layered materials are two-dimensional solids with strong bonding within the layers and weak bonding between them.[1] As a result they exhibit polytypism, which is often referred to as one-dimensional polymorphism, wherein layers stack one above the other in several ways yielding different polytypes with either ordered or random stacking.[2] For a given layered material, two of the three unit cell dimensions remain the same, and the third varies ranging from less than a nanometer to several hundred nanometers along the stacking direction, depending on the stacking sequence of the layers. For many layered materials, a small basic structure is the most common polytype.[3] Nevertheless, other polytypes with higher periodicity occur depending on the material. Among layered materials without interlayers, polytype diversity is limited, and is based on close packing considerations. However, among the materials with interlayers, formation of a polytype depends on several other factors including interlayer species, layer composition, and water content, leading to a larger diversity of polytypes.[4,5] In most cases laboratory syntheses of layered materials lead to disorder. Quite similar to polytypism, disorder in layered materials can also be seen as a consequence of anisotropic bonding and can be broadly classified into three kinds: turbostraticity, interstratifications, and stacking faults.[2] Cation vacancies and interstitials can complicate the picture.

Among inorganic layered materials, layered double hydroxides (LDH) are gaining considerable attention owing to their interesting properties and applications in several fields including catalysis, pigments, drug delivery, antacids, fire retardancy, and as sorbents.[6−9] They occur as minerals in several polytypic forms in nature and are important in the transport and sequestration of both cations and anions in the environment.[10] LDH are the opposite of cationic clays, in that LDH contain positively charged metal hydroxide layers with anions in the interlayer for charge compensation, while clays have negatively charged layers compensated by interlayer cations.[11] Anions in the interlayer of LDH are hydrated, and incorporation of excess water molecules into the interlayer could result in swelling, leading to exfoliation of these materials. While several anions ranging from monatomic halides to long chain surfactants can occupy the interlayer,[11] carbonate LDHs are most ubiquitous in nature.[12] Carbonate LDH are known to crystallize in two different polytypic modifications: hydrotalcite,

Received: December 2, 2014
Published: March 9, 2015

DOI: 10.1021/ic502820q
Inorg. Chem. 2015, 54, 3253−3259

a three-layer rhombohedral polytype ($3R_1$), and manasseite, a two-layer hexagonal polytype ($2H_1$).[13,14]

The $3R_1$ polytype has a metal hydroxide layer stacking sequence of AbC CaB BcA AbC···, and the $2H_1$ polytype has a stacking sequence of AbC CbA AbC···, where AbC stands for a metal hydroxide layer. The uppercase letters stand for the hydroxyl ion positions, and the lower case letters stand for the cation positions. The cation positions always correspond to the octahedral interstitials, and hence the layer can simply be represented as AC. A schematic representation of different polytypes is given in Figure 1.

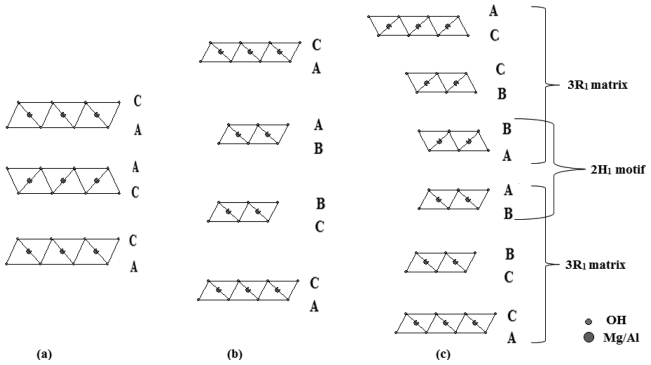

Figure 1. Schematic representation of (a) $2H_1$ polytype (b) $3R_1$ polytype (c) $3R_1$ polytype with $2H_1$ faults (interlayer is removed for clarity).

The layers in the $3R_1$ polytype are related by a stacking vector (2/3, 1/3, z), whereas, in the $2H_1$ polytype, the adjacent layers are related by a mirror-plane reflection. Both the polytypes are characterized by the presence of prismatic interlayers containing carbonate ions. Of these two, only the $3R_1$ polytype is realized in laboratory synthesis. However, often the laboratory syntheses of these materials results in disordered materials, which are replete with stacking faults, where the local symmetry of a fault resembles another polytype. For instance, a faulted material could have a stacking sequence AC CB BA AB BC CA AB BC···, where within a $3R_1$ matrix there is a fault whose local symmetry resembles the $2H_1$ polytype (Figure 1). The origin of stacking faults could be due to similar thermodynamic stabilities of different possible polytypes for a given material.[15] Polytype selection and disorder are mediated by intercalated anions and are also affected by water content in the interlayer and by the synthesis conditions.[16] Stacking faults in general are known to affect thermal, sorption, electrochemical, and mechanical properties of layered materials.[17,18] Thus, it is important to investigate the origin of disorder and study the energetics of formation of ordered and disordered structures. Here we determine the formation enthalpy of an ordered and a faulted Mg−Al LDH with interlayer carbonate, by direct measurement using high-temperature oxide melt solution calorimetry. Most of the above-mentioned properties are also affected by water molecules associated with LDH as mentioned earlier. It is, hence, crucial to determine the distribution of water molecules in LDH, and the enthalpy of hydration associated with water molecules present in different sites. Calorimetric measurements of water adsorption on the LDH aid in determining the enthalpy of water adsorption/hydration enthalpy and in evaluating the strength of binding of water molecules in LDH. In this work, we thus explore for the first time the energetics of formation of the two carbonate LDHs of similar composition from the perspective of their ordering, which has not been addressed in our earlier studies[19,20] and their water-adsorption energetics.

EXPERIMENTAL METHODS

Synthesis. Homogenous precipitation of mixed metal salts by urea hydrolysis is a well-known method to synthesize highly crystalline carbonate intercalated LDH[21] and was adopted in the present work. In a typical synthesis, 40 mL of mixed metal nitrate solution (total concentration, 0.5 M) containing ([Mg]/[Al]) = 2 was mixed with urea ([urea]/[total metal] = 3.5) and hydrothermally treated at 90 °C for 24 h in a Teflon liner sealed in a stainless steel autoclave. The resulting solid was washed with distilled water and dried at 60 °C. This sample is labeled as LDH 1. Faulted samples were prepared by the Riechle method,[22] which involves coprecipitation at constant high pH. In a typical synthesis, a mixed metal nitrate solution of required composition was slowly added to a solution containing 50 mL of NaOH (2M) and Na_2CO_3 (3 times the stoichiometric requirement) under constant stirring. The resulting slurry was aged at 70 °C for 18 h. The precipitate was separated by centrifugation and washed with distilled water to remove excess Na_2CO_3 and dried at 60 °C. The synthesized [Mg−Al−CO_3] LDHs are labeled as LDH 2 and LDH 3 corresponding to 2:1 and 3:1 ratios of [Mg]/[Al], respectively.

Characterization. Powder X-ray diffraction (XRD) of the synthesized samples were recorded using a Bruker AXS model D8 Advance diffractometer with Cu Kα radiation, Kα = 1.5418 Å, to determine the phases. The Rietveld technique was employed for structure refinement of the ordered phase using the GSAS software.[23] Structure refinement of the [Mg−Al−CO_3] LDH was performed using the published structure models (polytype $3R_1$: CC No. 6296; polytype $2H_1$: CC No. 182294). DIFFaX (Version 1.807)[24] was used to simulate XRD patterns of various polytypes and their intergrowths. Details of the application of this technique for simulation of the XRD patterns of polytypes and quantification of structural disorder are described elsewhere.[25]

The specific surface area was measured by the Brunauer−Emmett−Teller (BET) method using a Micromeritics Gemini VII surface area analyzer. The samples were degassed at 25 and 220 °C for 5 h before the measurements to obtain the surface area of hydrated LDH and dehydrated LDH, respectively. Thermogravimetric analysis (TGA) was performed to determine the water content in the samples using a Netzsch 449 thermal analysis system in dynamic Ar atmosphere (25−800 °C, 5 °C/min, Pt crucible). The data were analyzed using Netzsch Proteus software. The Mg and Al contents in the samples were measured by electron microprobe analysis using a Cameca SX 100 instrument operated at 15 kV with 10 mA probe current. Samples were pelletized, sintered, mounted on a probe holder, and polished with diamond paste. Fourier transform infrared attenuated total reflectance spectra (ATR-FTIR) of all the samples were recorded using a Bruker Model Alpha-P IR spectrometer (diamond ATR cell, 4 cm^{-1} resolution, 400−4000 cm^{-1}).

High-Temperature Oxide Melt Solution Calorimetry. High-temperature oxide melt solution calorimetry was performed using a custom-built isoperibol Tian-Calvet microcalorimeter as described by Navrotsky.[26,27] The calorimeter was calibrated using the heat content of high-purity α-Al_2O_3. Molten lead borate ($2PbO{\cdot}B_2O_3$) was used as solvent at 700 °C. Lead borate is toxic, and all the necessary precautions were taken while handling the molten solvent, which, however, does not have a significant vapor pressure at calorimeter temperature. The granular glass used as solvent had been melted commercially so we did not need to prepare it in our laboratory. Argon was flushed through the glassware at 60 mL/min to maintain constant atmosphere and bubbled through the solvent at 30 mL/min to remove liberated evolved gases, aid dissolution, and prevent local saturation of the solvent. In a typical experiment ~5 mg of sample were pelletized and dropped into the solvent. The resulting heat effect (heat of drop solution, ΔH_{ds}) includes the heat content of the sample, the heat effect associated with desorbing and vaporization of intercalated and adsorbed surface water, and the heat of dissolution of the sample in

DOI: 10.1021/ic502820q
Inorg. Chem. 2015, 54, 3253−3259

Table 1. Results of Compositional Analysis of [Mg−Al−CO_3] LDH

LDH sample	[Mg]/[Al]	total water content (mol)	intercalated water (mol)[a]	chemical formula
LDH 1	2	0.60	0.5	$[Mg_{0.67}Al_{0.33}(OH)_2][CO_3]_{0.166}\cdot 0.5H_2O$[b]
LDH 2	2	0.72	0.63	$[Mg_{0.66}Al_{0.34}(OH)_2][CO_3]_{0.17}\cdot 0.63H_2O$
LDH 3	2.9	0.57	0.35	$[Mg_{0.745}Al_{0.255}(OH)_2][CO_3]_{0.127}\cdot 0.29H_2O$

[a]Calculated using mass loss between 100 and 225 °C. [b]Carbonate content is given based on the measured Al content in the sample.

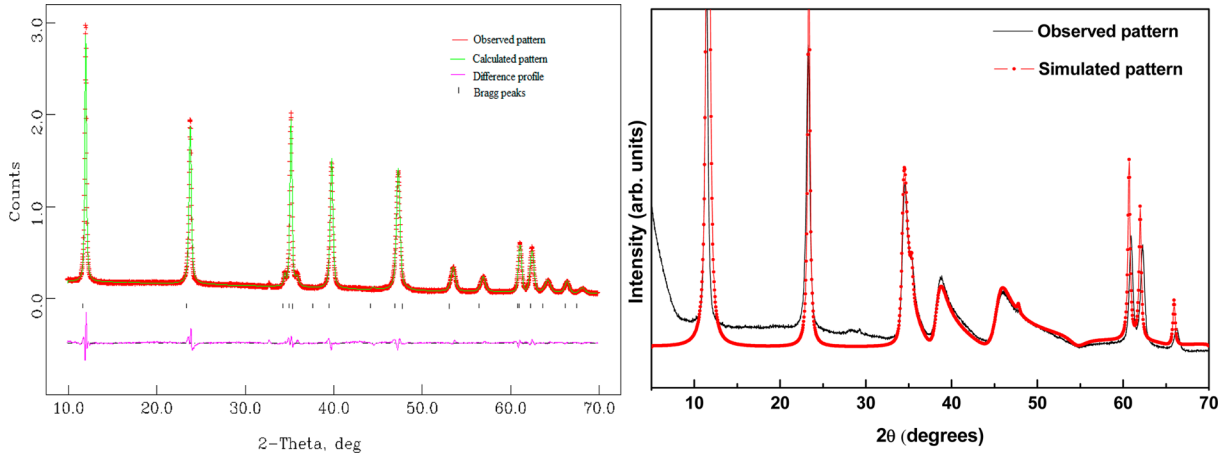

Figure 2. (a) Rietveld fit of the XRD pattern of LDH 1 and (b) PXRD pattern of LDH 2 overlaid with a simulated pattern corresponding to the $3R_1$ polytype with $2H_1$ stacking faults.

the high-temperature solvent. Heats of drop solution of the binary oxides, hydroxides, and metal carbonates were taken from previously published work.[28,29]

Water Adsorption Calorimetry. The instrument and methodology used for water adsorption calorimetry has been described elsewhere.[30] In a typical water adsorption calorimetric experiment ~25 mg of LDH was placed in a silica glass forked tube and was degassed at 220 °C under vacuum for 5 h using the degas port of a Micromeritics ASAP 2020 instrument. This was followed by measuring the enthalpy of adsorption of each incremental dose of water vapor using a coupled system consisting of the Micromeritics ASAP 2020 gas adsorption analyzer and a Setaram Sensys Calvet microcalorimeter. Each water dose (1 μmol) generates a distinct calorimetric peak due to heat effects associated with water adsorption, and the integral of area under the peak provides the corresponding heat of adsorption (differential enthalpy). The amount of water adsorbed until the differential enthalpy reaches the condensation enthalpy (−44 kJ/mol) of water is considered to be chemisorbed. The remaining water adsorbed at −44 kJ/mol is considered to be physisorbed. Throughout this work the reference state for water is the vapor, whose enthalpy does not depend on pressure at constant temperature since H_2O can be considered an ideal gas at these low pressures. A blank with an empty tube was run to correct the data for water adsorbed on the forked tube wall.

RESULTS AND DISCUSSION

Compositional analyses of all the LDHs are given in Table 1. The Mg/Al ratio of LDH 1, prepared by urea hydrolysis, and LDH 2, prepared by coprecipitation, was 2.0 in each case, and for LDH 3 that ratio was 2.9, which was close to the nominal composition. The carbonate content for all the samples was fixed based on the determined Al content.

The XRD pattern of LDH 1 exhibits sharp reflections indicative of a highly ordered sample. The Rietveld refinement of the PXRD pattern of this sample was done using the $3R_1$ structure model, and the fit is shown in Figure 2a. Acceptable goodness-of-fit parameters were obtained, and the results of refinements are given in Table 2. In the LDH 1 structure, O atoms of both carbonate and water molecules occupy the same

Table 2. Results of Rietveld Refinement of LDH 1

space group	$R\bar{3}mH$				
cell parameters, Å	a = 3.0413 (7); c = 22.656 (3)				
goodness-of-fit parameters	R_{wp} = 0.05; R_p = 0.04; $R(F^2)$ = 0.11; reduced χ^2 = 7.0				
refined atomic parameters					
atom	Wyckoff position	x	y	z	occupancy
Mg	3*a*	0.000	0.000	0.000	0.667
Al	3*a*	0.000	0.000	0.000	0.333
O1	6*c*	0.000	0.000	0.3771	1.0
C	6*c*	0.000	0.000	0.168	0.084
O2	18*h*	0.098	−0.098	0.168	0.5

18*h* site. Exactly above and below this 18*h* site, there are 6*c* sites, where the O atoms of the metal hydroxide layer reside, forming a prism. This arrangement of atoms promotes a strong hydrogen bonding of water molecules with the metal hydroxide layer. On the other hand XRD pattern of LDH 2 (Figure 2b) exhibits broad peaks indicative of disorder. However, the basal reflections (00*l*) and doublet at 60° 2θ (*hk*0 and *hkl*) characteristic of metal hydroxide layers are sharp, indicating the absence of interstratification and turbostraticity.[25] In the region between 30 and 55° 2θ there is asymmetric broadening of the peaks indicative of stacking faults.

A good fit of the observed pattern was obtained with a DIFFaX simulated pattern corresponding to the $3R_1$ polytype with 30% $2H_1$ stacking faults. However, it is important to note that the DIFFaX formalism, unlike the Rietveld technique, does not include a least-squares fit of the whole profile, but is a simple simulation of the XRD pattern of any given model structure that permits the inclusion of structural disorder and predicts the resultant line shape. The XRD pattern of LDH 3 (Supporting Information, Figure S1) shows similar broadening

DOI: 10.1021/ic502820q
Inorg. Chem. 2015, 54, 3253−3259

of reflections in the mid-2θ region indicative of stacking disorder.

IR spectra of all three LDHs confirm the presence of intercalated carbonate (Supporting Information, Figure S2) with a characteristic peak at 1360 cm^{-1}. While the metal nitrates were used for the synthesis of all the three LDHs, the possibility of nitrate being incorporated in the interlayer is very bleak. Carbonate can easily displace nitrate in the interlayer due to its high affinity for LDHs. O−H stretching vibration is observed at ∼3350−3360 cm^{-1}. TGA data were used to calculate the total water content present in the sample and the intercalated water content (Supporting Information, Figure S3). Mass loss observed up to 225 °C was used to calculate the total water content present in the LDH. The mass loss between 100 and 225 °C was used to calculate the intercalated water (Table 1), which was found to be 0.5, 0.63, and 0.35 mol for LDH 1, LDH 2, and LDH 3, respectively. Mass loss below 100 °C was attributed to adsorbed water. Differentiating intercalated water from physisorbed water in LDH is challenging, and in several cases it is indeed impossible. For instance, among oxyanions LDH other than carbonate, for example, sulfate and thiosulfate, intercalated water is generally known to desorb at temperatures as low as 40 °C.[31] In such cases TG data, even when coupled with mass spectrometry, cannot differentiate intercalated water from physisorbed water, and one can only estimate the total water content. On the other hand, in carbonate and halide LDHs, water loss below 100 °C has generally been attributed to physisorbed water.[32] Considering that the interlayer in the LDH is made of close-packed sites, parallel to the close-packed layers of metal hydroxide, with one crystallographic site per metal, the maximum amount of water that can be incorporated in the interlayer is given by $(1 - Nx/n)$ for the $[M^{II}_{1-x}M^{III}_{x}(OH)_2]^{x+}$ layer.[33] N is the number of sites occupied by an anion of charge n, and $(1 - Nx/n)$ will thus be the remaining sites that can be occupied by water or left vacant. For LDH 1 and LDH 2, where $x = 0.333$, the maximum amount of water that can be incorporated into an interlayer is therefore 0.5 mol per formula unit, while it is 0.625 mol for LDH 3 with $x = 0.745$. Water content calculated from TG mass loss (Table 1) thus indicates that the interlayer in LDH 1 is fully occupied, and in LDH 2 there is excess water in the interlayer, while in LDH 3 there are several vacant sites. Unlike in other oxo-anion LDHs where the anion is oriented perpendicular to the plane of the metal hydroxide layer, in carbonate LDHs the planar carbonate ions are oriented parallel to the plane of the metal hydroxide layers with water oxygens sharing same crystallographic sites with carbonate oxygens.[10] Thus, deviation from full occupancy of this crystallographic site might lead to disorder in the interlayer, which affects the stacking of layers. This might be one of the reasons for the observed stacking faults in LDH 2 and LDH 3, as opposed to LDH 1, which is highly ordered. Conversely, one could also argue that the stacking faults mediate incorporation of excess water in the case of LDH 2.

Water Adsorption Calorimetry. Figure 3 shows the differential enthalpies of water adsorption as a function of surface coverage of all three LDHs. The differential enthalpy of adsorption for the first dose at near zero coverage is −270.1, −264.4, and −254.7 kJ/mol for LDH 1, LDH 2, and LDH 3, respectively, indicating strong chemisorption of water on LDH. While the difference in the initial differential enthalpy of the three LDHs is not large in magnitude, the enthalpy is highest in magnitude for LDH 1, indicating that water is more strongly bound to carbonate when the interlayer is completely occupied and is ordered. With increasing surface coverage the differential enthalpies become less exothermic with successive doses before reaching the value of enthalpy of condensation of bulk water at 25 °C (−44 kJ/mol). The water adsorbed up to this coverage is strongly bound and is considered to be chemisorbed. Surface coverage of 28.4, 12.5, and 18.9 H_2O/nm^2 was observed for LDH 1, LDH 2, and LDH 3, respectively, when the differential enthalpy reached −44 kJ/mol. The amount of water adsorbed up to the coverage when the differential enthalpy of adsorption reached −44 kJ/mol for all three LDHs is given in Table 3. The sum of the differential enthalpies of adsorption divided by the total water content up to this coverage (integral enthalpy) corresponds to the enthalpy of chemisorbed water and is −97.2, −94.3, and −80.1 kJ/mol for LDH 1, LDH 2, and LDH 3, respectively.

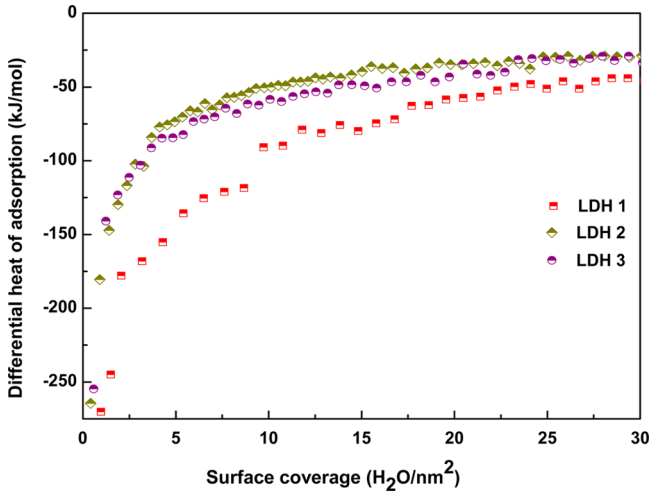

Figure 3. Water adsorption enthalpy curves of $[Mg-Al-CO_3]$ LDH.

Table 3. Calorimetric Data for Water Adsorption on $[Mg-Al-CO_3]$ LDH Degassed at 200 °C

sample	specific surface area (m^2/g)	differential enthalpy for first dose (kJ/mol)	surface coverage (H_2O/nm^2)[a]	integral enthalpy (kJ/mol)[a]	amount of water adsorbed (mol)[a]
LDH 1	30	−270.1	28.4	−97.2	0.098
LDH 2	82	−264.4	12.5	−94.3	0.11
LDH 3	76	−254.7	18.9	−80.1	0.159

[a]When the differential enthalpy reaches −44 kJ/mol.

The most negative enthalpy of chemisorption for LDH 1 indicates that water is more strongly bound in LDH 1 than on LDH 2. The integral enthalpy is least exothermic for LDH 3, which may be related to its lower carbonate content. The remaining water adsorbed with a differential enthalpy of −44 kJ/mol represents physically adsorbed water, which is loosely held. While the initial differential enthalpy and the integral enthalpy are similar for LDH 1 and LDH 2, the differential enthalpy at intermediate coverage is different as seen in Figure 3. This suggests that there are more energetically different sites available for the chemisorption of water in LDH 1, where the enthalpy of adsorption is more exothermic than in LDH 2.

Water molecules in LDH can exist in at least three different forms: (i) interlayer water, (ii) adsorbed water on the surface of the metal hydroxide layer, and (iii) free water between particles.

DOI: 10.1021/ic502820q
Inorg. Chem. 2015, 54, 3253−3259

Interlayer water further could be hydrogen bonded to (a) carbonate in the interlayer (forming the hydration sphere of the anion), where such bonding is expected to be stronger than the hydrogen bonding among water molecules that are not near the carbonate ion, or (b) to metal hydroxide layer. While there may be several structurally heterogeneous sites available for water molecules, it can be seen from Figure 3 that the differential enthalpy of water adsorption is a continuous function of water uptake, rather than a series of steps corresponding to the sequential filling of sites of different energies. This suggests a continuous and overlapping range of energies for the various sites. The initial highly exothermic water adsorption on all three LDH can be attributed to intercalated water hydrogen bonded to carbonate ions. This water can be removed only at 150−220 °C. However, the amount of water adsorbed on all three LDH (Table 3) when the differential enthalpy of adsorption reaches the value of −44 kJ/mol, is very low compared to the amount of intercalated water calculated from TG mass loss (Table 1). This indicates that not all of the water in the interlayer is strongly bound to carbonate ions. It is also known that carbonates do not exhibit large hydration enthalpies like sulfates, nitrates, and halides, which are known to grow their hydration sphere in the interlayer leading to the swelling of the LDH.[34,35] This raises an issue, whether the large differential enthalpy observed for the initial dose indeed corresponds to hydration of carbonate or the hydration of the unsaturated metal hydroxide surface of LDH or any amorphous metal hydroxides present, as cations (Mg/Al) are known to have large hydration enthalpies. Hydration of possible single cation phases in the sample, which would be X-ray amorphous or of low abundance, cannot be ruled out. To confirm that the initial hydration of LDH proceeds in the interlayer and not on metal hydroxide surfaces or amorphous hydroxide phases, if any, we performed water adsorption on LDH 1 degassed at room temperature. This gave an initial differential enthalpy of −142 kJ/mol as opposed to −270 kJ/mol observed when the LDH 1 is degassed at 220 °C, indicating that the former still contained some tightly bound water, presumably in the interlayer. However, the observed initial hydration enthalpy of −142 kJ/mol, when the sample is degassed at room temperature, also indicates that there is some chemisorbed water on the surface of the sample. These results, and the lower amount of chemisorbed water observed (Table 3) on completely dehydrated LDH (degassed at 220 °C), suggest that it is hard to differentiate between the adsorbed and intercalated water, as they overlap both energetically and in temperature of desorption. Thus, the initial adsorption is probably due to partial hydration of carbonate ions (presumably the first hydration sphere) and further possibly on the metal hydroxide surface, as we observe chemisorbed water when the sample is degassed at room temperature. Further hydration of the interlayer seems to be caused by physisorbed water. ^{1}H NMR and IR studies on [Mg−Al−CO_3] LDH have shown that water molecules in LDH are extensively hydrogen bonded.[36] On the basis of those studies it is concluded that the C_3 axis of the carbonate ions and the C_2 axis of water molecules in the interlayer are oriented parallel to the *c*-axis of the LDH, thereby restricting translational degrees of freedom of the water molecules. This is attributed to extensive hydrogen bonding of the water molecules in the interlayer. Our results show that the integral enthalpy of water adsorption on LDH is near −90 kJ/mol, indicating that some of the water molecules are strongly bound to LDH, which is in agreement with NMR studies. The rest of the water is loosely held in the interlayer and on the surface of the LDH. In an earlier report from our group, based on the difference in the energetics of formation of LDH computed from hydroxides, carbonates, liquid water, and from hydroxides, carbonate, ice, it was proposed that the water in LDH is in a unique state, which is intermediate in character between liquid water and solid ice.[28] On the basis of the associated entropy changes it was concluded that the water in LDH solid is not localized in an icelike state but possesses some rotational freedom in the interlayer. However, these water molecules do not have translational freedom like liquid water. Our current results are in agreement with this hypothesis, as we conclude that some water molecules are strongly bound, and some are loosely held in the LDH.

High-Temperature Oxide Melt Solution Calorimetry. Enthalpies of formation of all three LDHs were calculated from the oxides and from single cation hydroxides, carbonates, and water, using the thermochemical cycles shown in Table 4. The enthalpy data for the LDH phases and the reference phases used for calculation in the thermochemical cycle are given in Table 5. Enthalpy of drop solution values for all the reference phases were taken from previous reports.[28,29] Enthalpies of formation (see Table 5) calculated from oxides are −61.03 ± 1.85, −55.38 ± 2.11, and −51.65 ± 1.93 kJ/mol for LDH 1, LDH 2, and LDH 3, respectively. We observe stabilization of the ordered phase (LDH 1) compared to the faulted LDH (LDH 2) by a small difference in the enthalpy of formation (5.65 kJ/mol). Both LDH 1 and LDH 2 (x = 0.33) were found to be more stable than LDH 3 (x = 0.25).

Table 4. Thermochemical Cycles Used to Calculate Enthalpies of Formation of LDHs

from oxides (ΔH_f^{ox})[a]	
(1) $[Mg_{(1-x)}Al_x(OH)_2][(CO_3)_{x/2}\cdot mH_2O]$ (s, 298) → (1 − x) MgO(soln, 973) + x/2 Al_2O_3 (soln, 975) + x/2 CO_2 (g, 975) + (1 + m)H_2O (g, 973)	$\Delta H_{dsol,1}$
(2) (1 − x) MgO (s, 298) → (1 − x)MgO (soln, 975)	$\Delta H_{dsol,2}$
(3) x/2Al_2O_3 (s, 298) → x/2Al_2O_3 (soln, 975)	$\Delta H_{dsol,3}$
(4) (1 + m)H_2O (s, 298) → (1 + m) H_2O (g, 975)	$\Delta H_{dsol,4}$
(5) x/2 CO_2 (g, 298) → x/2 CO_2 (g, 975)	$\Delta H_{dsol,5}$
(6) (1 − x)MgO (s, 298) + x/2 Al_2O_3 (s, 298) + x/2 CO_2 (s, 298) + (1 + m)H_2O (l, 298) → $Mg_{1-x}Al_x(OH)_2(CO_2)_{x/2}\cdot mH_2O$ (s, 298)	$\Delta H_{f,ox}$
[a] $\Delta H_{f,ox} = -\Delta H_{dsol,1} + \Delta H_{dsol,2} + \Delta H_{dsol,3} + \Delta H_{dsol,4} + \Delta H_{dsol,5}$	
from single cation hydroxides and salt (ΔH_f^{scc}) and water[b]	
$Mg_{(1-x)}Al_x(OH)_2$ $(CO_3)_{x/2}\cdot mH_2O$(cr, 298 K) → (1−3/2x) $Mg(OH)_2$ (soln, 975 K) + (x/2)$MgCO_3$ (soln, 975 K) + $xAl(OH)_3$ (soln, 975 K) + mH_2O (g, 975 K)	$\Delta H_{dsol,1}$
$Mg(OH)_2$ (s, 298 K) → $Mg(OH)_2$ (soln, 975 K)	$\Delta H_{dsol,2}$
$MgCO_3$ (s, 298) → $MgCO_3$ (soln, 975 K)	$\Delta H_{dsol,3}$
$Al(OH)_3$ (s, 298 K) →$Al(OH)_3$ (soln, 975 K)	$\Delta H_{dsol,4}$
H_2O (l, 298 K) → H_2O (g, 975 K)	$\Delta H_{dsol,5}$
[b] $\Delta H_{f,ch} = -\Delta H_{dsol,1} + (1 - 3/2x)\Delta H_{dsol,2} + (x/2)\Delta H_{dsol,3} + x\Delta Hd_{sol,4} + m\Delta H_{dsol,5}$	

A cobalt aluminum carbonate intercalated LDH was earlier found to have an enthalpy of formation close to zero from the corresponding binary hydroxides, carbonates, and water.[19] However, in several other cases, depending on the cation and the water content, LDHs were found to be significantly more stable than the mechanical mixtures of hydroxides and carbonates.[20] In the present case the enthalpy of formation from single cation hydroxide, carbonate, and water is −16.03 ±

DOI: 10.1021/ic502820q
Inorg. Chem. 2015, 54, 3253−3259

Table 5. Enthalpies of Drop Solution (ΔH_{dsol}) and Enthalpies of Formation from Oxides ($\Delta H_{f,ox}$) and from Carbonates, Hydroxides, and Water ($\Delta H_{f,SCC}$)

sample	ΔH_{dsol} (kJ/mol)	$\Delta H_{f,ox}$ (kJ/mol)	$\Delta H_{f,SCC}$ (kJ/mol)
MgO	37.93 ± 2.11		
Al_2O_3	108.62 ± 0.99		
H_2O (l)[a]	69.0		
CO_2[a]	32.07		
$Mg(OH)_2$	144.35 ± 1.04	−37.42 ± 2.35	
$Al(OH)_3$	184.56 ± 0.97	−26.75 ± 1.08	
$MgCO_3$	186.70 ± 1.44	−116.7 ± 2.55	
LDH 1	215.12 ± 1.21 (8)[b]	−63.05 ± 1.85	−16.03 ± 1.25
LDH 2	218.93 ± 1.85 (10)[b]	−57.29 ± 2.11	−10.17 ± 1.83
LDH 3	190 ± 2.34 (9)[b]	−51.65 ± 1.93	−7.1 ± 2.16

[a]Calculated from heat capacity. [b]Values in () indicate number of experiments.

1.25, −10.17 ± 1.83, and −7.1 ± 2.16 kJ/mol for LDH 1, LDH 2, and LDH 3, respectively. The ordered LDH 1 is the most stable followed by disordered LDH 2 (x = 0.33) and LDH 3 (x = 0.25). Our measurements thus show that the ordered LDH is energetically more stable. It is also presumably more stable in free energy, since stacking faults, not being three-dimensional, introduce negligible entropy. Nevertheless, most laboratory syntheses result in disordered LDH replete with stacking faults, and some mineral samples are also found to be intergrowths of two polytypes. The reasons for this behavior may be kinetic and mechanistic rather than thermodynamic. While there could be several possibilities, we discuss here two different possible reasons for the formation of the faulted phase.

Several factors affect the LDH phase formation during synthesis, including hydrolysis of cations in the solution and the pH and temperature of precipitation. In the present case, LDH 1 was synthesized by urea hydrolysis, which provides homogeneous precipitation. During the urea hydrolysis there is in situ generation of base (NH_3) and carbonate ion, which interact with metal ions in the solution resulting in the formation of the LDH phase. The rate of urea hydrolysis, and thus the resulting pH in the solution, can be easily controlled by controlling the temperature. Such controlled conditions during synthesis lead to homogeneous precipitation and uniform crystal growth. These result in formation of an ordered phase as observed in the case of LDH 1. On the other hand LDH 2 and LDH 3 were prepared by ammonia precipitation, where mixed metal nitrate solution was added to a solution containing required amounts of NaOH and Na_2CO_3. Here the synthesis conditions are not controlled, other than by the rate of addition of metal nitrate solution. Hydrolysis of cations to precipitate the LDH phase is thus rapid, unlike in the case of LDH 1 where it is slow and controlled. Kinetic factors are thus crucial during the precipitation of LDH phase from aqueous phase, and thus might dictate the formation of ordered versus faulted LDH.

Carbonate, whose molecular symmetry is D_{3h}, matches the local symmetry of the prismatic interlayer (D_{3h}) as opposed to the octahedral interlayer (D_{3d}), and carbonate LDH in nature crystallizes in $3R_1$ and $2H_1$ polytypes with prismatic interlayers.[13,14] However, laboratory synthesis of $2H_1$ polytype has not been reported, and most syntheses result in faulted material as mentioned earlier. Stacking faults are one-dimensional disorder. These faults, once formed, cannot be eliminated by hydrothermal treatment. Simulation of XRD pattern of LDH 2 fits the $3R_1$ polytype with 20% $2H_1$ faults, as mentioned in text earlier. While the interlayers are similar in both $2H_1$ and $3R_1$ polytypes, they do differ in cation arrangements in the adjacent layers, which are superimposed in the case of $2H_1$ along the c-direction and are displaced by (2/3, 1/3) in the case of $3R_1$. In the $2H_1$ polytype the adjacent metal hydroxides are related by reflection (AC CA AC---), but it is by a simple translation in the $3R_1$ polytype (AC CB BA AC---). Both of these factors suggest that the formation of the $2H_1$ polytype requires higher activation energy than the formation of the $3R_1$ polytype, and the latter is often observed in laboratory synthesis. This kinetic and mechanistic argument can also be supported by the observation that hydrotalcite ($3R_1$) and manasseite ($2H_1$) often occur together in minerals, with the latter on the inside and the former on the outside of the grains, suggesting that the formation of $2H_1$ is favored by high temperature.[37] Thus, it could be possible that stacking faults mediate polytype transformation from $3R_1$ to $2H_1$ and are themselves not kinetically labile. It is also known in several cases that stacking faults are related to phase transformations as they fundamentally represent a transition between two well-defined phases/polytypes.[3] The extent of transition depends on the quantity and distribution of faults. Thus, the formation and observation of faults is kinetic in origin.

LDH phases are known to crystallize in a wide composition range ($0.2 \leq x \leq 0.4$).[6] Distribution of the cations in the layers with different composition is often a topic of debate.[38] It is often postulated that x = 0.33 with [Mg]/[Al] = 2 is cation ordered due to a cation avoidance rule, and thus it is more favorable to form LDH phases devoid of impurities.[39] Any sample that deviates from this composition is assumed to either have a random arrangement of cations with the constraint that the trivalent (Al) cations are distributed as far as possible from each other ($0.20 < x < 0.33$) or result in impurities along with the LDH phase ($x > 0.33$). From our experiments we observe that change in composition of the LDH layer with varying x also results in a difference in formation enthalpy, where LDH 1 and LDH 2 having x = 0.33 are more stable than LDH 3 having x = 0.25 by 11.4 and 5.64 kJ/mol, respectively. While this energy difference is small, the two LDHs with x = 0.33 are thermodynamically more stable, which could possibly be due to cation ordering in the layer. In the laboratory synthesis, a composition preference is not seen in Mg−Al LDH, and it is known to form the LDH phase in a wide composition range ($0.2 \leq x \leq 0.4$). This possibly could be attributed to the observed energy difference, which is not large enough. LDHs are precipitated in aqueous phases, and it is more likely that the relative activities of cations, pH, and temperature of the solution dictate the composition and the phase of the LDH formed.

CONCLUSION

We have examined the energetics of ordered and faulted Mg−Al LDH with carbonate ions in the interlayer. The ordered LDH is thermodynamically more stable than the faulted LDH by ∼6 kJ/mol. Without a large thermodynamic driving force, the frequent formation and observation of faulted samples is likely to be kinetic in origin. Synthesis conditions including pH, temperature, and rate of hydrolysis of cations affect the structure of the LDH phase. Stacking faults could also be kinetically nonlabile, but they might nevertheless mediate transition between pure polytypes. Water molecules present in the LDH also significantly affect the properties of LDH

DOI: 10.1021/ic502820q
Inorg. Chem. 2015, 54, 3253−3259

including their structure. Water adsorption calorimetry on LDH shows a continuous decrease in the magnitude of adsorption enthalpy with water content, indicating the presence of a continuum of energetically heterogeneous sites for H_2O.

■ ASSOCIATED CONTENT

Supporting Information

PXRD pattern of the LDH 3 (x = 0.25), IR spectra of all the three LDHs, and TG-DTG curves of all the three LDHs. This material is available free of charge via the Internet at http://pubs.acs.org.

■ AUTHOR INFORMATION

Corresponding Author

*E-mail: anavrotsky@ucdavis.edu.

Notes

The authors declare no competing financial interest.

■ ACKNOWLEDGMENTS

This work was supported by the U.S. Department of Energy, Office of Basic Energy Sciences, Grant No. DE-FG02-97ER14749.

■ REFERENCES

(1) Verma, A. R.; Krishna, P. *Polymorphism and Polytypism in Crystals;* John Wiley: New York, 1966.
(2) Baumhauer, H. *Z. Kristallogr.* **1912**, *50*, 33.
(3) Trigunayat, G. C.; Verma, A. R. Polytypism and Stacking Faults in Crystals with Layered Structures. In *Crystallography and Crystal Chemistry of Materials With Layered Structures;* Levy, F., Ed.; Reidel Publishing Company: Dordrecht, The Netherlands, 1976.
(4) Tessier, C.; Haumesser, P. H.; Bernard, P.; Delmas, C. *J. Electrochem. Soc.* **1999**, *146*, 2059−2067.
(5) Radha, S.; Prasanna, S. V.; Kamath, P. V. *Cryst. Growth Des.* **2011**, *11*, 2287−2293.
(6) Evans, D. G.; Duan, X. *Chem. Comm.* **2006**, 485−496.
(7) Choy, J. H.; Kwak, S. Y.; Park, J. S.; Jeong, Y. J.; Portier, J. *J. Am. Chem. Soc.* **1999**, *121*, 1399.
(8) Cavani, F.; Trifiro, F.; Y, J.; Vaccari, A. *Catal. Today* **1991**, *11*, 173.
(9) Prasanna, S. V.; Kamath, P. V. *Solid State Sci.* **2008**, *10*, 260−266.
(10) Drits, V. A., Bookin, A. S. Crystal Structure and X-ray Identification of Layered Double Hydroxides. In *Layered Double Hydroxides: Present and Future;* Rives, V., Ed.; Nova Science: New York, 2001; p 39.
(11) Brindely, G. W.; Kikkawa, S. A. *Am. Mineral.* **1979**, *64*, 836.
(12) De. Roy, A.; Forano, C.; Besse, J. P. Layered Double Hydroxides: Synthesis and Post Synthesis Modification. In *Layered Double Hydroxides: Present and Future;* Rives, V., Ed.; Nova Science: New York, 2001; pp 1−39.
(13) Taylor, W. F. *Mineral. Mag.* **1969**, *30*, 377−389.
(14) Chao, G. Y.; Gault, R. A. *Can. Mineral.* **1997**, *35*, 1541−1549.
(15) Tripathi, M. N.; Waghmare, U. V.; Ramesh, T. N.; Kamath, P. V. *J. Electrochem. Soc.* **2010**, *157*, A280−A284.
(16) Radha, S.; Kamath, P. V. *Cryst. Growth Des.* **2009**, *9*, 3197−3203.
(17) Ramesh, T. N.; Kamath, P. V. *Mater. Res. Bull.* **2008**, *43*, 2827−2832.
(18) Radha, S.; Navrotsky, A. *J. Phys. Chem. C* **2014**, *118*, 29836−29844.
(19) Allada, R. K.; Navrotsky, A. N.; Berbeco, H. T.; Casey, W. H. *Science* **2002**, *296*, 721−723.
(20) Allada, R. K.; Peltier, E.; Navrotsky, A.; Casey, W. H.; Johnson, C. A.; Berbeco, H. T.; Sparks, D. L. *Clays Clay Miner.* **2006**, *54*, 409−417.
(21) Hibino, T.; Ohya, H. *Appl. Clay Sci.* **2009**, *45*, 123−132.
(22) Reichle, W. T. *Solid State Ionics* **1986**, *22*, 135−141.
(23) Larson, A. C.; Von Dreele, R. B. *General Structure Analysis System (GSAS);* Technical Report LAUR 86−748 for the Los Alamos National Laboratory: Los Alamos, NM, 2004.
(24) Treacy, M. M. J.; Deem, M. W.; Newsam, J. M. Computer Code DIFFaX, v. 1.807, 2000; http://www.public.asu.edu/~mtrecy/DIFFaX.html.
(25) Radha, A. V.; Shivakumara, C.; Kamath, P. V. *Clays Clay Miner.* **2005**, *53*, 521−528.
(26) Navrotsky, A. *Phys. Chem. Miner.* **1977**, *2*, 89−104.
(27) Navrotsky, A. *Phys. Chem. Miner.* **1997**, *24*, 222−241.
(28) Allada, R. K.; Navrotsky, A.; Goates, J. B. *Am. Mineral.* **2005**, *90*, 329−335.
(29) Navrotsky, A. *J. Am. Ceram. Soc.* **2014**, *97*, 3349−3359.
(30) Ushakov, S. V.; Navrotsky, A. *Appl. Phys. Lett.* **2005**, *87*, 164103.
(31) Radha, S.; Antonyraj, C. A.; Kamath, P. V.; Kannan, S. *Z. Anorg. Allg. Chem.* **2010**, *636*, 2658−2664.
(32) Constantino, V. R. L.; Pinnavia, T. J. *Inorg. Chem.* **1995**, *34*, 883−892.
(33) Ingram, L.; Taylor, H. F. W. *Mineral. Mag.* **1967**, *36*, 465−479.
(34) Antonyraj, C. A.; Koilraj, Pand.; Kannan, S. *Chem. Commun.* **2010**, *46*, 1902.
(35) Iyi, N.; Fujji, K.; Okamoto, K.; Sasaki, T. *Appl. Clay Sci.* **2010**, *35*, 218−227.
(36) Van der Plo, A.; Mojet, B. L.; Vandeven, E.; Deboer, E. *J. Phys. Chem.* **1994**, *98*, 4050−4054.
(37) de la Calle, C.; Pons, C. H.; Roux, J.; Rives, V. *Clays Clay Miner.* **2003**, *51*, 121−132.
(38) Sideris, P. J.; Nielsen, U. G.; Grey, C. P. *Science* **2008**, *321*, 113−117.
(39) Evans, D. G.; Slade. R. C. T. Structural Aspects of Layered Double Hydroxides. In *Layered Double Hydroxides;* Duan, X., Evans, D. G., Eds.;Springer: New York, 2005.

DOI: 10.1021/ic502820q
Inorg. Chem. 2015, 54, 3253−3259